# Quantum interference in $SiO_2$: A conduction-band mass reappraisal

R. Ludeke[a)] and H. J. Wen
*IBM T. J. Watson Research Center, P.O. Box 218, Yorktown Heights, New York 10598*

Andreas Schenk
*Integrated Systems Laboratory, Swiss Federal Institute of Technology, Gloriastrasse 35, CH-8092 Zürich, Switzerland*

(Received 19 February 1998; accepted for publication 30 June 1998)

Quantum oscillations arising from interference in over-the-barrier injected electrons crossing a metal–oxide–semiconductor structure were observed for a 2.8 nm $SiO_2$ layer. Model calculations that include image force effects are fitted to the data to obtain a conduction-band mass of $m_{ox} = (0.63 \pm 0.09) m_0$. The field dependence of the oscillations was used to deduce the polarity and magnitudes of oxide charge induced by the high fluence of electrons injected with the scanning tunneling microscope during spectral acquisitions. © *1998 American Institute of Physics.* [S0003-6951(98)01535-6]

We report in this letter the determination of the conduction-band effective-mass $m_{ox}$ in $SiO_2$ gate oxides from interference oscillations in the over-the-barrier current of electrons injected into a metal–oxide–semiconductor (MOS) structure with a scanning tunneling microscope (STM). Electron wave or quantum interference in the thin oxide layer of MOS structures during Fowler–Nordheim (F–N) injection was predicted by Gundlach in 1966.[1] A weak oscillatory structure in the F–N current was observed by Maserjian and Petersson in 1974,[2,3] and subsequently by others,[4–8] from which values of $m_{ox}$ in the range of 0.32 (Ref. 1) to $0.85 m_0$ (Refs. 2 and 6) were estimated from Gundlach's treatment of transmission through a trapezoidal barrier.[1] This treatment neglects barrier modifications due to image force effects. Values of $m_{ox}$ from $0.3 m_0$ (Ref. 9) to $0.5 m_0$(Ref. 10) were also estimated from fits of the F–N current expression to experiment, with $m_{ox}$ as the fitting parameter. For these fits the tenuous assumptions were made that besides the neglect of image force effects, the other parameters, such as the oxide thickness, barrier height, and oxide field, in the exponent of the F–N current expression are precisely known. A value of $0.5 m_0$ is now generally accepted and used in transport simulations.[11] The stated sources of uncertainties and other inherent problems of F–N methods, such as a position-dependent electron energy due to the high fields, suggest a reassessment of this issue, particularly in view of the availability of novel experimental approaches. Many of the limitations of F–N-based determinations of $m_{ox}$ are overcome in this work by using the localized injection scheme of the STM-based ballistic electron emission microscopy (BEEM). From an analysis of the observed quantum oscillations in the BEEM current traversing the oxide we determine a value of $m_{ox} = 0.63 \pm 0.9 m_0$, and furthermore, illustrate the potential use of quantum interference to assess local charge variations in ultrathin oxides.

In BEEM the STM tip is used to inject electrons into the metal gate of a MOS structure, from where they may enter directly into the conduction band of the $SiO_2$ provided their energy exceeds the barrier height $eV_{th}$ at the M–O interface.[12] A schematic energy-band diagram of the BEEM experiment is shown in the inset of Fig. 1. The tip bias $V_T$ is referenced to the metal gate so that $eV_T$ represents the kinetic energy of the electrons. When $eV_T \geqslant eV_{th}$, which defines the threshold energy for electron transmission and thereby the dynamic potential maximum in the oxide, a finite collector current $I_c$ emerges from the Si substrate. By dynamic is meant the potential sensed by the injected electrons as modified by screening effects, described by image force theory, arising from both cladding layers surrounding the $SiO_2$. This barrier is shown as a solid curve in the inset. The static (trapezoidal) barrier is depicted by the dashed line and includes a built-in oxide potential of 0.2 V that is attributed to the work-function differences between the Pd gate and $n$-type Si.[13] An optionally applied bias voltage $V_b$ between gate and Si was set to zero. Details of the BEEM experiment are given elsewhere.[12,13]

The 2.8 nm $SiO_2$ layers used in this work were thermally

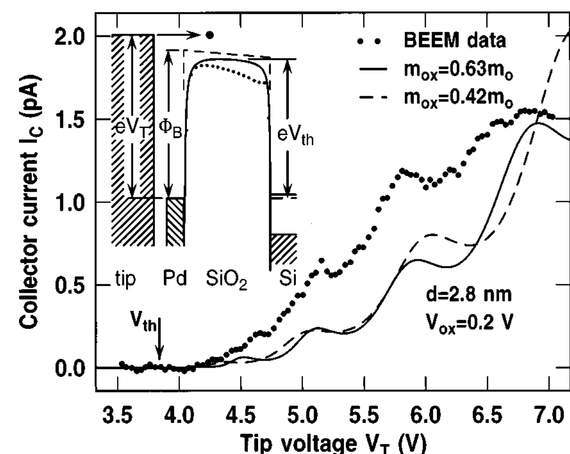


FIG. 1. Composite BEEM spectrum (dots) obtained on virgin areas of a 2.8 nm oxide. The solid and dashed line are "simulated" spectra. The inset shows an energy-band diagram for the experiment with potential barrier depicted in the presence (solid) and absence of image force effects (dashed line). The dotted profile includes a positive oxide charge of $3 \times 10^{13}/cm^2$ 0.4 nm from the Si interface. $I_T = 2$ nA, $V_b = 0$.

a)Electronic mail: ludeke@watson.ibm.com

 © 1998 American Institute of Physics

grown near 800 °C in dry oxygen on 125 mm Si(100) wafers (phosphorus doped to $\sim 10^{16}$ cm$^{-3}$). $\sim 8\times 15$ mm$^2$ pieces were cleaved from the wafer and outgassed in ultrahigh vacuum (UHV) at 250 °C prior to being covered with ~4–5 nm thick Pd dots, 0.2 mm in diameter, that were thermally evaporated through a shadow mask. The finished sample was then transferred under UHV into the STM chamber. BEEM data were acquired in sets consisting of nine spectra evenly spread over a $100\times 100$ nm$^2$ area. The quoted thickness $d$ was determined ellipsometrically on similarly annealed pieces immediately after their removal from UHV. Estimated error for $d$ is $\pm 0.2$ nm.

The dotted curve in Fig. 1 is an average over five sets of spectra each taken on a virgin or previously unexposed portion of the sample surface. An average is shown to improve statistics. This particular oscillatory behavior is reproducible and is observed in 30%–40% of the spectra taken. The structure in the remaining spectra is generally weaker or undistinguishable from the noise. As we had previously shown, the mere injection of charge in a BEEM experiment can fill existing electron traps and even create them at high tip biases ($V_T > 6$ $V$) in oxides with $d > 4$ nm,[14] or produce observable positive charge in thinner oxides.[15] As we will discuss later, such oxide charges have a clearly observable effect on the oscillatory structure. Suffice to say for now that the structure depicted in Fig. 1 is representative of a portion of oxide that is essentially charge free during most if not all of the first scan at a virgin spot. In order to avoid charging effects from prior injections the new acquisition site needed to be some 10 nm or more away from any previously exposed spot.

The oscillatory structure is attributed to quantum interference effects in the thin $SiO_2$ layer, which arise from the constructive/destructive interference of electron waves reflected at the metal– $SiO_2$ and $SiO_2$–Si boundaries of the $SiO_2$ ''cavity.'' For the simplest case of a rectangular barrier, maxima in the over-the-barrier transmission coefficient obey the quantization condition:

$$E=(n\pi\hbar/d)^2/2m^* \quad (n=1,2,3,\dots), \tag{1}$$

where $E$ is the electron energy, $d$ the cavity width, and $m^*$ the effective electron mass.[1] However, the presence of an internal field, screening effects, and a more realistic treatment of the interfaces alter these quantization conditions.[16,17] We have incorporated these more realistic features in calculating the transmission coefficient $T(E)$ by numerical solution of the one-dimensional Schrödinger equation.[17] We assume a parabolic dispersion within the oxide with the momentum taking the form:

$$k(x)=\sqrt{2m_{\rm ox}/\hbar^2}\ \sqrt{E-[\Phi_B+eF_{\rm ox}x+E_{\rm im}(x)]}, \tag{2}$$

where, $E_{\rm im}$ is the image potential that includes the effect of all images in the two electrodes,[16] $\Phi_B$ is the barrier height, and $F_{\rm ox}$ is the oxide field. Following the approach by Ando and Itoh for an arbitrary potential barrier,[18] we divide the barrier depicted in the inset of Fig. 1 into $N$ equal segments with coordinate $x_l$ marking the $l$th segment. With boundary conditions of continuity of both wave function and quantum-mechanical current density at each boundary the $T(E)$ is then found to be

$$T(E)=\frac{m_0}{m_{N+1}}\frac{k_{N+1}}{k_0}\frac{|\det M|^2}{|M_{22}|^2}, \tag{3}$$

where $M$ is a $(2\times 2)$ product matrix $M=\Pi_{l=0}^{N}M_l$ with transfer matrices $M_l(x_l)$ being only functions of momentum $k_l$ and effective-mass $m_l$ in the $l$th segment.[18] With the metal–oxide interface at $x_0$ and the oxide–silicon interface at $x_N$, $m_0=m_M$ denotes an effective mass in the metal electrode and $m_N=m_{\rm Si}$ the ''effective'' mass in silicon. For all other $l$ we have $m_l=m_{\rm ox}$, although a variable, energy dependent $m_l$ could be incorporated as well. In our simulations the following parameters were used: $d=2.8$nm, $N=30$, $\Phi_B=4.1$ eV,[13] $F_{\rm ox}=V_{\rm ox}/d=0.07143$ V/nm (potential peak at the oxide–metal boundary),[13] and $m_{\rm Si}=0.19\,m_0$, $m_M=m_0$, $\epsilon_{\rm Si}=11.7$, and $\epsilon_{\rm ox}=2.13$.

$T(E)$ is a rapidly rising function for $E > eV_{\rm th}$ that exhibits an oscillatory structure with maxima near unity.[1,17,18] In order to make the connection with experiment, we have chosen to simply ''simulate'' a BEAM spectrum by multiplying $T(E)$ with a simple quadratic power law, i.e., $I_c \propto (eV_T - eV_{\rm th})^2$, an assumption often made in the threshold region,[19] but of limited applicability at higher energies in $SiO_2$, where scattering effects commence to dominate in thicker layers.[12] The results of this exercise are shown for two different masses $m_{\rm ox}$ in Fig. 1, with the solid curve clearly giving the superior fit to the data, as judged from the position of the maxima. Image force effects are included in both curves. The sensitivity of the position of the maxima on $m_{\rm ox}$ can be estimated by differentiating Eq. (1), giving $\delta m_{\rm ox}=-(\delta E/E)m_{\rm ox}$. Thus, a $\delta E=0.1$ eV gives a $\delta m_{\rm ox}=0.01m_0$ for $E=6$ eV. Our best estimate for the uncertainty in $E$ gives an error of $\pm 0.02m_0$. In contrast, the error in $d$ of $\pm 0.2$ nm, yields the much larger uncertainty of $\pm 0.09m_0$.Other uncertainties in the estimates of $V_{\rm ox}$ ($< \pm 0.1$ V) or in the choice of $\epsilon_{\rm ox}$ give uncertainties of $< 0.01m_0$, so that our present best estimate for $m_{\rm ox}$ is $m_{\rm ox}=(0.63\pm 0.09)m_0$. Ignoring image force effects, a best fit to the experimental data gives a $m_{\rm ox}\approx 0.65m_0$. However, we find no physical reason for this omission.

We will next readdress the issue of local charge on the interference structure. To study this, we sequentially acquired a series of spectra taken at the same point of the sample, with each spectral acquisition further stressing the oxide. A few spectra of such a sequence are shown in Fig. 2. The digit next to the curves indicates the number of the spectral scan. The first scan shows the strong modulation of the oscillator current at a virgin spot on the surface, in agreement with the spectrum shown in Fig. 1. The subsequent scan is already substantially modified in both the strength and position of the interference maxima. Further changes in structure are observed in succeeding spectra. A second point to be noted is the progressive increase in the collector current $I_c$ with the third and subsequent scans. These increases are attributed to the buildup of stress-induced positive charge near the anode (O–S interface) of thin oxides,[15] a process also invoked to explain current increases with electron fluence in F–N stressed MOS capacitors.[20] The positive charge creates an accelerating field that results, with the inclusion of image force effects, in an enhancement of transmission probabilities and an increase in $I_c$.[21]

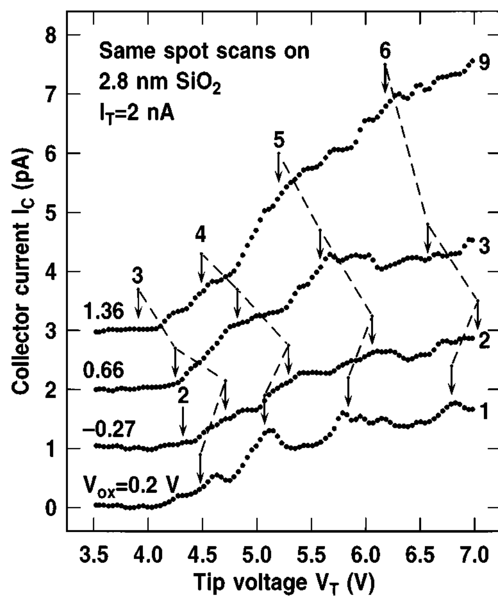


FIG. 2. Single scan BEEM spectra on a 5 nm Pd/2.8 nm $SiO_2/n$-Si(100)MOS structure measured at the same point on the sample. The numerals on the right of the spectra indicate the number of the scan. The first spectrum was taken on a previously unexposed area of the sample. Arrows mark the theoretical position of interference maxima for the indicated oxide potentials. Maxima of the same order are linked by a dotted line. The spectra are vertically displaced for clarity. $I_T = 2$ nA, $V_b = 0$ V.

We illustrate the modification of the potential in the inset of Fig. 1, where the dotted curve represents the calculated profile due to the presence of a hypothetical positive charge density of $3\times10^{13}/\text{cm}^2$ placed 0.4 nm from the O–S interface.[14] An assumed randomness in the distribution of the charge and its buildup during repeated scanning (i.e., stressing[15]) progressively distorts the local potential, thereby affecting the ability of the electron waves to interfere coherently. Consequently, electrons injected locally near an area of charge would experience both a local- and time-dependent variation of the fields, which leads to a reduction of the interference effects, as was observed in Fig. 2, or frequently to total suppression (not shown). Nevertheless, an ''average'' oxide potential may be estimated from the interference structure through fits to $T(E)$. The locations of interference maxima from solutions of Eq. (3), with values of $V_{ox}$ that constitute a best visual fit indicated on the left of the spectra, are shown by arrows above each spectrum. The dashed lines connect the same order of the interference, which is indicated above the top spectrum. The increasing value of $V_{ox}$ obtained from these fits is consistent with the buildup of positive charge stipulated previously to account for the increase in $I_c$ with stress. An interesting exception is the second scan, whose interference structure could only be fitted by assuming a retarding oxide field, that is, an initial presence of negative charge. A retarding field shifts the oscillations to higher energy, which enhances the observation of the next lower order peak (2) in the spectrum. The presence of trapped negative charge had previously been verified through both increases in the threshold voltage and decreases of $I_c$ of stressed thicker (>4 nm) oxides.[14] On thinner oxides a stress-induced increase in $I_c$, coupled with a lack of clear threshold shifts, was attributed to the presence of positive charge, with any trapped electrons leaking out.[15] However, the interference data of Fig. 2 now indicate that some of the trapped negative charge is retained, at least initially, and is observable prior to the slower buildup of the positive charge with stress. Threshold shifts are more difficult to ascertain in the presence of both interference structure and the increased noise of a single scan, although spectrum 2 in Fig. 2 does suggest a ~0.2 V increase in $V_{th}$ as compared to scan 1. An estimate of the charge density responsible for generating the average $V_{ox}$ deduced from the interference structure can be made using a sheet charge model.[14] Assuming that the charge centroids for the negative[14] and positive charges are $0.5d$ and $0.2d$, respectively, from the O–S interface, local charge densities of $-0.9$, $+1.7$, and $+4.4\times10^{13}/\text{cm}^2$ were estimated to cause the interference structure in spectra 2, 3, and 9, respectively.

We conclude that the observation of interference effects in BEEM is an opportunity to reassess local over-the-barrier transport in dielectrics in order to determine the bounds of relevant fundamental parameters, the effective conduction-band mass $m_{ox}$ of $SiO_2$ in the present case. The sensitivity of the interference to local electric fields in the oxide can be used to assess the polarity and distribution of intrinsic and/or stress-induced local charge. However, the ready trapping and charge generation in the oxides may be somewhat of an impediment to the assessment of spatial variations in oxide parameters on a highly resolved scale.

[1] K. H. Gundlach, Solid-State Electron. **9**, 949 (1966).
[2] J. Maserjian and G. P. Peterson, Appl. Phys. Lett. **25**, 50 (1974).
[3] J. Maserjian, J. Vac. Sci. Technol. **11**, 996 (1974).
[4] M. V. Fischetti, D. J. DiMaria, L. Dori, J. Batey, E. Tierney, and J. Stasiak, Phys. Rev. B **35**, 4044 (1987).
[5] J. C. Poler, K. K. McKay, and E. A. Irene, J. Vac. Sci. Technol. B **12**, 88 (1994).
[6] S. Zafar, K. A. Conrad, Q. Liu, E. A. Irene, G. Hames, R. Kuehn, and J. J. Wortman, Appl. Phys. Lett. **67**, 1031 (1995).
[7] S. Zafar, Q. Liu, and E. A. Irene, J. Vac. Sci. Technol. A **13**, 47 (1995).
[8] H. S. Momose, M. Ono, T. Yoshitomi, T. Ohguru, S. Nakamura, M. Saito, and H. Iwai, IEEE Trans. Electron Devices **45**, 1233 (1996).
[9] T. Yoshida, D. Imafuku, J. L. Alay, S. Miyazaki, and M. Hirose, Jpn. J. Appl. Phys., Part 2 **34**, L903 (1995).
[10] Z. A. Weinberg, J. Appl. Phys. **53**, 5052 (1982).
[11] M. V. Fischetti, S. E. Laux, and E. Crabbé, J. Appl. Phys. **78**, 1058 (1995), and references therein.
[12] R. Ludeke, A. Bauer, and E. Cartier, Appl. Phys. Lett. **66**, 730 (1995); J. Vac. Sci. Technol. B **13**, 1830 (1995).
[13] H. J. Wen, R. Ludeke, D. M. Newns, and S. H. Low, J. Vac. Sci. Technol. A **15**, 784 (1997).
[14] H. J. Wen and R. Ludeke, J. Vac. Sci. Technol. B **15**, 1080 (1997); R. Ludeke and H. J. Wen, Appl. Phys. Lett. **71**, 3123 (1997).
[15] H. J. Wen and R. Ludeke, J. Vac. Sci. Technol. A **16**, (1998).
[16] A. Schenk and G. Heiser, J. Appl. Phys. **81**, 7900 (1997).
[17] H. J. Wen, R. Ludeke, and A. Schenk (unpublished).
[18] Y. Ando and T. Itoh, J. Appl. Phys. **61**, 1497 (1987).
[19] W. J. Kaiser and L. D. Bell, Phys. Rev. Lett. **60**, 1406 (1988); L. D. Bell and W. J. Kaiser, *ibid.* **61**, 2368 (1988).
[20] D. Buchanan, D. J. DiMaria, C. A. Chang, and Y. Taur, Appl. Phys. Lett. **65**, 1820 (1994).
[21] E. Cartier, R. Ludeke, and H. J. Wen (unpublished results).